

Studying the γ -ray pulsar J1932+1916 and its pulsar wind nebula with *Chandra*

O D Medvedev¹, A V Karpova¹, Yu A Shibano¹, D A Zyuzin¹ and G G Pavlov²

¹Ioffe Institute, Politekhnicheskaya 26, St. Petersburg, 194021, Russia

²Pennsylvania State University, 525 Davey Lab., University Park, PA 16802, USA

E-mail: medvedev.oleg12@gmail.com

Abstract. We report on the results of *Chandra* X-ray observations of the γ -ray radio-quiet pulsar J1932+1916. We confirm the previous detection of the pulsar counterpart and its pulsar wind nebula in X-rays from low spatial resolution data obtained by *Suzaku* and *Swift*. The *Chandra* data with much better spatial resolution resolved the fine structure of the nebula in the pulsar vicinity, which can be interpreted as jets bent by the ram pressure. The size of this compact part is about $30''$, and it is surrounded by a weak asymmetric diffusive emission extended up to $\approx 2'.8$. The X-ray spectra of the pulsar, the compact and extended parts of the nebula can be described by the power-law models with photon indexes of $0.44^{+0.57}_{-0.61}$, $2.34^{+0.95}_{-0.79}$ and $2.14^{+0.32}_{-0.31}$, respectively. The actual pulsar's X-ray flux is several times weaker than it was obtained with *Suzaku* and *Swift* where it was dominated by the unresolved nebula. We discuss possible associations of J1932+1916 with the nearby supernova remnant G54.4-0.3.

1. Introduction

To date *Fermi* γ -observatory has detected 234 pulsars (see, e.g., <https://confluence.slac.stanford.edu/di>). Several dozens of them are radio-quiet, which makes X-ray observations particularly important for further studies of their properties.

The γ -ray radio-quiet pulsar J1932+1916 (hereafter J1932) was discovered in a ‘blind search’ of the *Fermi* data [1]. The pulsar has the following parameters: R.A.= $19^{\text{h}}32^{\text{m}}19^{\text{s}}70(4)$, Dec.= $+19^{\circ}16'39''(1)$ (hereafter, numbers in parentheses are 1σ uncertainties in the last digits quoted unless stated otherwise), the period $P = 208$ ms, the characteristic age $\tau = 35$ kyr, the spin-down luminosity $\dot{E} = 4 \times 10^{35}$ erg s⁻¹, the magnetic field $B = 4.5 \times 10^{12}$ G and the γ -ray flux above 100 MeV $G_{100} = 7.8(4) \times 10^{-11}$ erg cm⁻² s⁻¹.

First X-ray observations of the J1932 field with the *Swift* and *Suzaku* telescopes revealed a possible pulsar counterpart as well as a presumed pulsar wind nebula (PWN) [2]. However, low spatial resolution of the instruments did not allow us to study the objects in detail. To confirm the J1932 counterpart candidate and to clarify the properties of the pulsar+PWN system, we performed new observations with *Chandra*, which provides the best spatial resolution in X-rays. Here we present the results of the observations.

2. X-ray data and imaging

Two 15-ks *Chandra* ACIS-I observations of the J1932 field were carried out on 2018 February 26 and 28 (ObsIDs 20742 and 20986; PI G. Garmire). The data were reprocessed and analysed

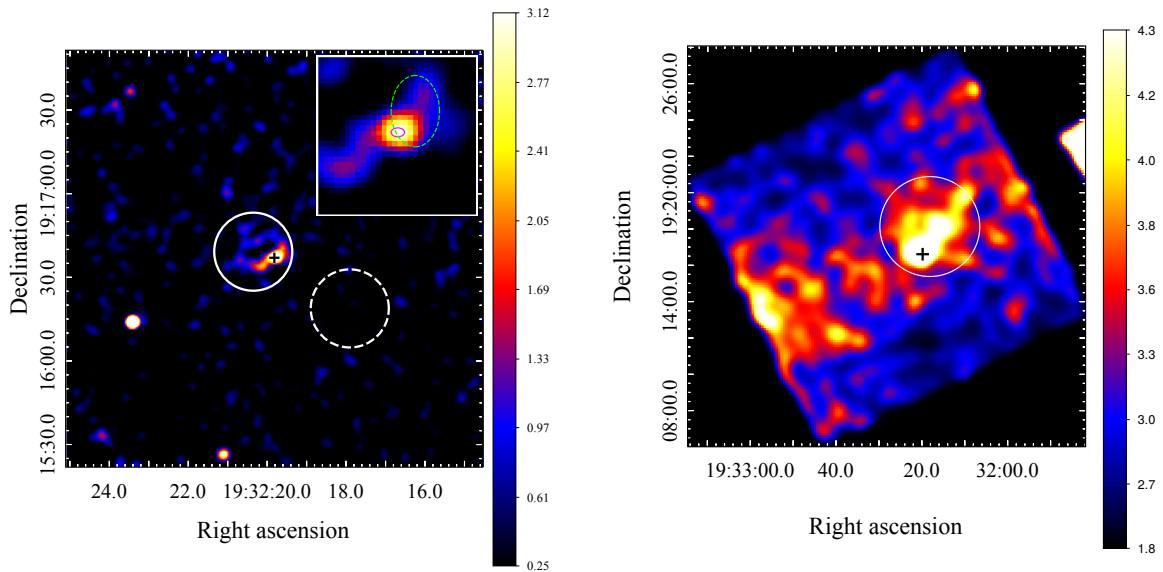


Figure 1. *Left:* $2'5 \times 2'5$ exposure-corrected *Chandra* ACIS-I image of the J1932 field in the 0.5–7 keV band smoothed with a 6 pixel Gaussian kernel (1 pixel = $0''.5$). The intensity is given in 10^{-8} photon cm^{-2} s^{-1} pixel^{-1} . The likely pulsar counterpart position is shown by the cross. The solid and dashed circles were used for the extraction of the compact PWN and background spectra, respectively. The internal box show the zoomed-in $15'' \times 15''$ region around the J1932 counterpart candidate smoothed with a 5 pixel Gaussian kernel. The green dashed and magenta solid ellipses show 3σ position uncertainties of J1932 in γ -rays and the presumed X-ray counterpart, respectively. The green ellipse combines the *Fermi* position uncertainties and the *Chandra* astrometric accuracy (the latter is estimated from 90% confidence *Chandra* aspect solution accuracy of $0''.8$; see <http://cxc.cfa.harvard.edu/cal/ASPECT/celmon/>). *Right:* Exposure-corrected image of the ACIS-I FOV in the 0.5–7 keV band smoothed with a 6 pixel Gaussian kernel (1 pixel = $8''$). The intensity is given in 10^{-7} photon cm^{-2} s^{-1} pixel^{-1} . The $2'75$ -radius circle marks the large-scale nebula emission around J1932. Extended emission near the south-east edge of the FOV is likely associated with the shell of SNR G54.4–0.3.

using CIAO v.4.11 package. The exposure-corrected image of the pulsar vicinity is shown in the left panel of figure 1 where the data from the two sets were combined. A point-like source is seen at the γ -ray position of J1932 as well as a weak compact nebula around it, which resembles two bent tails (or jets). The point source position obtained with the *wavdetect* tool on the merged image is R.A.= $19^{\text{h}}32^{\text{m}}19^{\text{s}}.817(15)$ and Dec.= $+19^{\circ}16'37''.00(14)$ where errors in brackets are pure statistical uncertainties.

To search for a large-scale X-ray emission in the pulsar field, previously observed with *Suzaku* [2], we created the image where point-like sources were excluded. The resulting holes were filled with background counts taken from annuli regions around the sources using the *dmfilth* tool. The image of the ACIS-I field-of-view (FOV) is presented in the right panel of figure 1. One can see some extended diffuse emission around J1932 which may be a fainter part of its PWN. Its size is about $5'.5$. It coincides with the extended source (the presumed PWN) detected with *Suzaku*. The surface brightness of the latter can be described by the 2D Gaussian model with $\text{FWHM} \sim 4'.5$ [2]. Note that diffuse emission south-east of the pulsar (near the ACIS-I edge) may be related to the supernova remnant (SNR) G54.4–0.3 which was proposed as the J1932 host remnant [2].

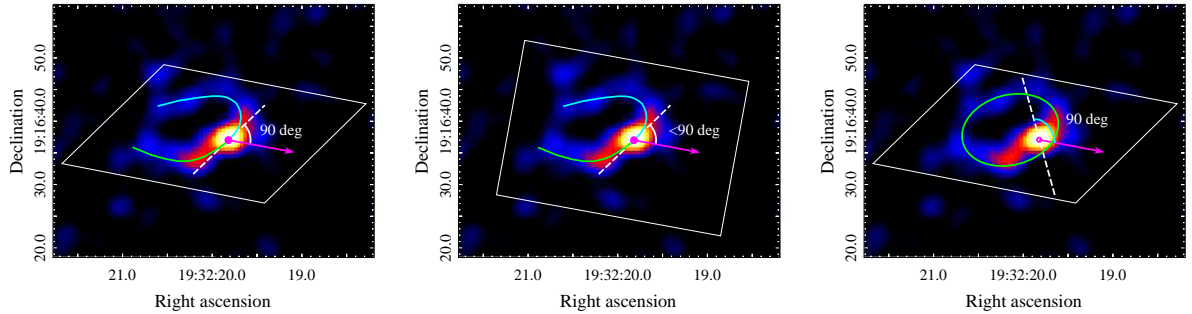


Figure 2. $50'' \times 40''$ ACIS-I images of the pulsar field in the 0.5–7 keV band encapsulating the compact nebula part. Possible geometries of the system are shown. The assumed pulsar’s proper motion (p.m.) direction and its spin axis are shown by the magenta arrow and the white dashed line, respectively. White tetragons indicate the plane of the system. In the left and middle panels the green and cyan lines represent jets bent by the ram pressure. In the right panel the green ellipse shows the equatorial outflow (torus) shifted by the ram pressure. See text for details.

3. Spectral analysis

The X-ray spectra in both datasets are extracted using `specextract` task. For the J1932, we use the $2''$ -radius aperture, while the $14''$ -radius circle with the pulsar aperture subtracted is used for the compact PWN (figure 1). The background spectra are extracted from the dashed circle. For each object, spectra are combined to increase signal-to-noise ratio and grouped to ensure at least 1 count per energy bin. We obtain 19 and 83 total source counts from J1932 and its nebula, respectively. Due to the low count number, we use C -statistics [3] to fit the data. We fit the compact nebular (CN) spectrum containing more source counts in the 0.5–10 keV band using `XSPEC v.12.9.1` and the absorbed power law (PL) model. We obtain the following best-fit parameters (hereafter all errors correspond to 1σ confidence intervals): the absorbing column density $N_{\text{H}} = 1.36_{-0.78}^{+1.08} \times 10^{22} \text{ cm}^{-2}$, the photon index $\Gamma^{\text{CN}} = 2.34_{-0.79}^{+0.95}$, the unabsorbed flux in the 0.5–8 keV band $F_{\text{X}}^{\text{CN}} = 1.0_{-0.4}^{+1.8} \times 10^{-13} \text{ erg cm}^{-2} \text{ s}^{-1}$ and $C = 65.7$ (degrees of freedom d.o.f. = 96). We fit the J1932 counterpart candidate spectrum fixing the column density at the best-fit value for the PWN. The PL model fit is: $\Gamma^{\text{PSR}} = 0.44_{-0.61}^{+0.57}$, unabsorbed flux $F_{\text{X}}^{\text{PSR}} = 2.2_{-0.5}^{+0.6} \times 10^{-14} \text{ erg cm}^{-2} \text{ s}^{-1}$ and $C = 14.2$ (d.o.f. = 16). The black body (BB) model for the pulsar suggests a temperature of $1.4_{-0.4}^{+0.8} \text{ keV}$ which is too large for the entire surface of a neutron star (NS) or for its hot polar caps (see e.g. [4]).

We analyze the extended nebula (EN) spectrum using the circle region shown in the right panel of figure 1 to extract the spectrum (the $14''$ -radius circle used for the compact PWN analysis was excluded as well as point-like sources). We grouped the spectrum to ensure 20 counts per energy bin and used χ^2 -statistics. We fit this spectrum fixing the column density at the best-fit value for the compact PWN. The PL model results in $\Gamma^{\text{EN}} = 2.14_{-0.31}^{+0.32}$, unabsorbed flux $F_{\text{X}}^{\text{EN}} = 8.3_{-1.1}^{+1.3} \times 10^{-13} \text{ erg cm}^{-2} \text{ s}^{-1}$ and $\chi^2 = 228$ (d.o.f. = 199).

4. Discussion and conclusions

The J1932 X-ray counterpart flux measured from *Chandra* data is by a factor of 5 smaller than that obtained in [2]. It is clear now that the latter was dominated by the compact PWN structures around the pulsar which were not resolved by *Suzaku* and *Swift*. The ratio of the pulsar fluxes in γ -rays and X-rays is $\log(G_{100}/F_{\text{X}}^{\text{PSR}}) \approx 3.5$ which is in agreement with the value typical for the radio-quiet γ -ray pulsar population [5].

The derived photon indices indicate that the PWN emission appears to be softer than that

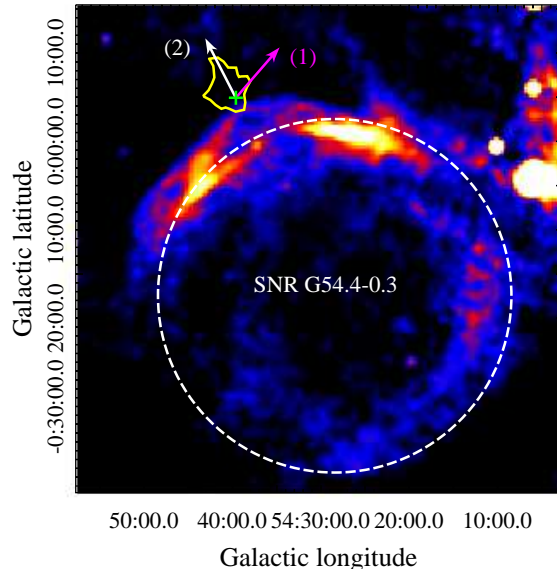


Figure 3. Image of the SNR G54.4–0.3 obtained from the VGPS. The J1932 X-ray counterpart position is marked by the green cross. The magenta arrow (1) indicates the pulsar p.m. as shown in figure 2. The white arrow (2) shows the pulsar’s p.m. in the case of its association with G54.4–0.3. The yellow contour corresponds to the boundary of the large-scale PWN emission around J1932 seen in the right panel of figure 1.

of the pulsar. The column density N_{H} is in agreement with the value obtained in [2] though it is too uncertain to better constrain the distance to the pulsar. The unabsorbed flux from the extended nebula is compatible with the value obtained for the entire PWN seen in the *Suzaku* data [2].

The J1932 compact nebula may be similar to the ‘lateral tails’ observed in the PWN of PSRs J0633+1746 (Geminga) and J1509–5850 [6, 7, 8]. These tails could represent a limb-brightened shell formed by the ram pressure of the ISM interacting with the pulsar wind. The shape of such a shell may be a body of rotation with the symmetry axis along the pulsar’s p.m. direction. A deficit of diffuse emission between the tails in this case can be caused by magnetic field dependence of the azimuthal angle around the shell axis [7]. This explanation seems to be implausible for J1932 due to observed asymmetry of the compact nebula. However, the axially asymmetric shell is expected if the pulsar’s p.m. direction and spin axis are not aligned, and the pulsar wind is concentrated in the equatorial plane [7]. For example, if the spin axis is perpendicular to the p.m. direction and the plane of the sky, two bent streams without emission between them could be observed.

There is another interpretation of ‘lateral tails’ as jets or an equatorial torus bent back by the ram pressure [6, 7, 8]. We show possible geometries in figure 2. The system asymmetry can be explained as follows: the plane of the system defined by the p.m. and spin vectors can be not perpendicular to the line of sight (figure 2, left and right) or the spin axis can be not perpendicular to the pulsar’s p.m. direction (figure 2, middle).

All the geometries for J1932 system shown in figure 2 assume the same direction of the pulsar p.m. As was noted above, J1932 can be associated with the SNR G54.4–0.3 [2]. The radio image of the latter obtained from the VLA Galactic Plane Survey (VGPS) [9] is presented in figure 3. The association of J1932 and G54.4–0.3 requires the pulsar’s p.m. direction (the white arrow

in figure 3) very different from that one indicated in figure 2. Thus, the geometries assumed in figure 2 reject the association.

Recently, a $\sim 5''$ -radius ring structure was detected around the presumed pulsar CXOU J061705.3+222127 (J0617) in the SNR IC 443 [10]. The center of the ring is offset by $2''.7$ from the J0617 position. This may be explained either as an intrinsic azimuthal asymmetry provided by nonuniform circumstellar medium or as a geometric effect due to a shift of the ring from the equatorial plane [10]. The same situation can take place for J1932. In this case its p.m. direction is unclear, and we cannot exclude G54.4–0.3 as the host remnant, presuming the p.m. direction of J1932 along the white arrow in figure 3. The large scale PWN (right panel of figure 1), whose extent is shown by the yellow contour in figure 3, appears to be stretched along this arrow, suggesting some protrusion ahead of the pulsar.

Deeper observations are necessary to clarify the nature of the small- and large-scale PWN structures around J1932. Detection of the proper motion and X-ray pulsations from J1932 could help to understand geometry of the system and its association with G54.4–0.3.

Acknowledgments

GGP acknowledges support from the ACIS Instrument Team contract SV4-74018 issued by the Chandra X-ray Observatory Center, which is operated by the Smithsonian Astrophysical Observatory for and on behalf of NASA under contract NAS8-03060. The ACIS Guaranteed Time Observations included here were selected by the ACIS Instrument Principal Investigator, Gordon P. Garmire, of the Huntingdon Institute for X-ray Astronomy, LLC, which is under contract to the Smithsonian Astrophysical Observatory; Contract SV2-82024. For figure 3 we used the data from the VGPS survey conducted by the National Radio Astronomy Observatory (NRAO) instruments. NRAO is a facility of the National Science Foundation operated under cooperative agreement by Associated Universities, Inc. DAZ thanks Pirinem School of Theoretical Physics for hospitality.

References

- [1] Pletsch H J *et al.* 2013 *ApJ* **779** L11
- [2] Karpova A, Shternin P, Zyuzin D, Danilenko A and Shibano Y 2017 *MNRAS* **466** 1757–63
- [3] Cash W 1979 *ApJ* **228** 939–47
- [4] Viganò D, Rea N, Pons J A, Perna R, Aguilera D N and Miralles J A 2013 *MNRAS* **434** 123–41
- [5] Abdo A A *et al.* 2013 *ApJS* **208** 17
- [6] Kargaltsev O, Pavlov G G, Klingler N and Rangelov B 2017 *Journal of Plasma Physics* **83** 635830501
- [7] Posselt B *et al.* 2017 *ApJ* **835** 66
- [8] Klingler N, Kargaltsev O, Rangelov B, Pavlov G G, Posselt B and Ng C Y 2016 *ApJ* **828** 70
- [9] Stil J M *et al.* 2006 *AJ* **132** 1158–76
- [10] Swartz D A *et al.* 2015 *ApJ* **808** 84